Persistence Length of Carboxymethyl Cellulose As Evaluated from Size Exclusion Chromatography and Potentiometric Titrations

C. W. Hoogendam, A. de Keizer,* M. A. Cohen Stuart, and B. H. Bijsterbosch

Laboratory of Physical Chemistry and Colloid Science, Wageningen Agricultural University, P.O. Box 8038, 6700 EK Wageningen, The Netherlands

J. A. M. Smit and J. A. P. P. van Dijk

Department of Physical and Macromolecular Chemistry, Leiden University, P.O. Box 9502, 2300 RA Leiden, The Netherlands

P. M. van der Horst

Akzo Nobel Chemicals Arnhem, Westervoortsedijk 73, P.O. Box 9300, 6800 SB Arnhem, The Netherlands

J. G. Batelaan

Akzo Nobel Central Research Arnhem, Velperweg 76, P.O. Box 9300, 6800 SB Arnhem, The Netherlands

Received July 14, 1997; Revised Manuscript Received June 1, 1998

ABSTRACT: The intrinsic persistence length of carboxymethyl cellulose (CMC) is determined by size exclusion chromatography in combination with multiangle laser light scattering (SEC−MALLS) as well as from potentiometric titrations. Samples with degree of substitution (ds) ranging from 0.75 to 1.25 were investigated. The relation between molar mass M and radius of gyration R_g as obtained by SEC−MALLS is determined in 0.02, 0.1, and 0.2 mol L^{-1} $NaNO_3$. Using the electrostatic wormlike chain theory a bare (intrinsic) persistence length L_{p0} of CMC is assessed at 16 nm, irrespective of the degree of substitution. A somewhat lower value (12 nm) is obtained when Odijk's theory for the description of polyelectrolyte dimensions is applied. The difference between L_{p0} assessed from both models is discussed briefly. Potentiometric titrations were carried out in NaCl solutions (ranging from 0.01 to 1 mol L^{-1}). From the titrations the radius of the CMC backbone was obtained by application of the model of a uniformly charged cylinder. The radius amounts to 0.95 nm for CMC ds = 0.75, and increases to 1.15 nm for CMC with ds = 1.25. The pK for the intrinsic dissociation constant of the carboxyl groups (i.e., at zero degree of dissociation) amounted to 3.2. L_{p0} was also deduced from potentiometric titrations. A model developed by Katchalsky and Lifson, which relates the dissociation behavior of a polyelectrolyte to the stiffness of its chain, was applied to CMC. From analyses of the potentiometric titrations an intrinsic persistence length of 6 nm was deduced. The difference between L_{p0} assessed from SEC−MALLS and potentiometric titrations is discussed briefly.

Introduction

The macroscopic properties of polymer solutions are determined by microscopic (molecular) parameters. For example, the viscosity of a polymer solution is influenced by the molar mass of the polymer, its radius of gyration R_g, and its flexibility. Thickening properties of a polymer solution are related to the rigidity of the polymer backbone, which is characterized by the persistence length L_p. Knowledge of microscopic parameters is also required to describe polymer adsorption at a solid−liquid interface. A general finding is the preferential adsorption of molecules with large molar mass,[1] implying that for a polydisperse polymer the composition of the mixture, i.e., the molar mass distribution, is of importance. Although at present little is known about the influence of the local stiffness on the adsorption properties of polymers, its effect on solution properties is generally recognized. Polymers having equal molar masses will be more extended when they have a higher persistence length. The larger extension manifests itself in a slower motion (diffusion) of the molecule.

For many years, viscometry has been applied as a method to determine the persistence length. By measuring the concentration dependence of the viscosity the intrinsic viscosity of a polymer solution is determined. The intrinsic viscosity is related to the dimension and the molar mass of a polymer. As the former is related to the persistence length, viscometry enables determination of L_p. However, the molar mass must be determined separately (e.g., by means of the Mark−Houwink relation). Furthermore, quantities obtained by viscometry are averages. So, for (nearly) monodisperse polymers, viscometry might be used as a suitable technique to determine L_p, but if applied to polydisperse samples, additional information about the molar mass distribution is needed. Information about the distribution is accessible from size exclusion chromatography (SEC). In this technique, which is also known as gel permeation chromatography (GPC), molecules are separated according to their size, yielding the molar mass distribution.

Cellulose derivatives are well-known for their thickening properties. In this connection, most cellulose compounds are characterized by a persistence length in the range 5−20 nm.[2] In this paper we focus on the

S0024-9297(97)01032-2 CCC: $15.00
Published on Web 08/15/1998

determination of the persistence length of carboxymethyl cellulose (CMC). As CMC is a polyelectrolyte, repulsion between charged segments will affect the persistence length; i.e., L_p will depend on the degree of dissociation of the polyelectrolyte and on the salt concentration. Hence, the parameter that characterizes the local stiffness originating from the polymer backbone is the magnitude of L_p in the absence of any electrostatic effects. It is denoted as the *bare* or *intrinsic* persistence length L_{p0}. From viscometry Rinaudo[3] obtained $L_{p0} = 5.0$ nm at high salt concentrations where electrostatic interactions are negligible. L_p was calculated from the intrinsic viscosity according to Yamakawa et al.[4] The same value is obtained by Kamide et al.[5] who applied various theoretical models (Benoit−Doty[6] and Yamakawa[4]) to published viscosity data. A value of 8.5 nm was obtained by Lavrenko et al.[7] from viscosity measurements of CMC solutions in mixtures of water and cadoxen (Cd^{2+}−ethylenediamine complex).

We used size exclusion chromatography in combination with multiangle laser light scattering (SEC−MALLS) to determine the intrinsic persistence length of CMC. The use of light scattering as the detection method for SEC offers the possibility of analyzing a polymer sample in terms of the distribution of molar mass and molecular dimensions. The latter is represented by the radius of gyration R_g. The advantage of light scattering over viscometry as the detection method is that with the former M_w and R_g are determined in an absolute way, i.e., unlike viscometry where a calibration is needed to relate the detector signal to the required quantity. CMC samples with different numbers of substituted groups per monomeric unit (degree of substitution, ds, from 0.75 to 1.25) and molar masses ($30-10^3$ kg mol^{-1}) were prepared from the same cellulose source by a homogeneous substitution reaction. By this approach a well-defined set of CMC samples is obtained so that the relation between M and chain dimensions can be determined as a function of ds over a broad range of M. The relation between M and R_g reveals information about the persistence length of a polymer. The electrostatic wormlike chain model is used to analyze this relation and to determine L_{p0}. In our analysis we follow the approach proposed by Davis.[8] Besides Davis's approach we will discuss our data in terms of Odijk's model.[9] The two approaches yield somewhat different values for the intrinsic persistence length. We will discuss briefly the difference between L_{p0} values obtained from the two models.

In addition to SEC−MALLS the CMC samples were characterized with respect to their dissociation behavior by means of potentiometric titrations. The latter were interpreted in terms of a uniformly charged cylinder, which serves as a model for a CMC molecule on a length scale of L_p. In this way information about the cross-section of the CMC backbone is obtained. Potentiometric titrations were also used to estimate L_{p0}. For this purpose a modified analysis proposed by Katchalsky[10,12] was used.

Theoretical Background

Electrostatic Wormlike Chain Model. First, the theory describing the dimensions of a (charged) wormlike polyelectrolyte will be briefly outlined. For a more comprehensive review of the electrostatic wormlike chain model, the reader is referred to a paper by Davis.[8]

The size of a macromolecule in solution is often characterized by its radius of gyration R_g. This quantity measures the root-mean-square distance of the segments from the center of mass of the chain. For a linear flexible homopolymer, R_g can be calculated to a first approximation from the random walk model. Dividing the chain into N_K segments each of length L_K (Kuhn length), the radius of gyration for a random chain is given by[13]

$$R_{g0}^2 = \frac{1}{6} N_K L_K^2 \tag{1}$$

In the random walk model, excluded volume effects are neglected; R_g calculated in this manner is called the unperturbed radius of gyration R_{g0}. Equation 1 only applies to a chain for which the length scale L_p of the local stiffness is small compared to the length of the stretched chain (contour length L_c). More generally, the unperturbed dimension of a chain can be expressed in terms of L_p and L_c by means of the wormlike chain model:[14a]

$$R_{g0}^2 = L_c^2\left[\frac{1}{3}x - x^2 + 2x^3 - 2x^4(1 - e^{-1/x})\right] \tag{2}$$

where $x = L_p/L_c$. Equation 2 is quite general, it includes (as limits) both the Gaussian coil and the rigid rod. It can be shown that for long wormlike chains $L_K = 2L_p$.[14a] Then the limit corresponding to the former (eq 1) is recovered when $L_c/L_p \gg 1$. For the other limit (rigid rod) the equation approaches $R_{g0}^2 = {}^1/_{12} L_c^2$, namely when $L_c/L_p \ll 1$ (i.e., if bending between adjacent segments is not allowed). In eq 2 the mutual interaction between polymer segments and interaction between segment and solvent is not taken into account (i.e., excluded volume effects are neglected). Excluded volume effects are taken into account by introducing a linear expansion factor (α_{ev}). The dimension of the chain is written as a product of the unperturbed dimension and the chain expansion factor: $R_g = \alpha_{ev} R_{g0}$. Since R_g is composed of two parameters (R_{g0} and α_{ev}), this approach is often denoted as the two-parameter model. In general, α_{ev} depends on the molar mass, the local stiffness of the chain, and the solvent quality. In a Θ-solvent α_{ev} is unity; the mutual attraction between segments is exactly counterbalanced by repulsive interactions between segments. If repulsion between segments prevails, a chain will adopt a more extended conformation: $\alpha_{ev} > 1$. The linear expansion factor is a function of the excluded volume parameter z. We will use the expression for α_{ev} derived by Yamakawa and Tanaka:[14b]

$$\alpha_{ev}(z) = [0.541 + 0.459(1 + 6.04z)^{0.46}]^{1/2} \tag{3}$$

The expression for z in case of a wormlike chain is[15]

$$z = \frac{1}{32}\left(\frac{3}{\pi L_p^2}\right)^{3/2}\left(\frac{L_c}{L_p}\right)^{1/2}\beta\frac{3}{4}K(N_K) \tag{4}$$

where β is the excluded volume per Kuhn segment. The function $K(N_K)$ reflects the probability of contact between Kuhn segments in a chain. For a Gaussian chain ($N_K \gg 1$) $K(N_K)$ has a limiting value ${}^4/_3$, so that ${}^3/_4 K(N_K) = 1$. For $N_K \to 0$, $K(N_K)$ becomes zero.[15,16] Hence, the function $K(N_K)$ takes into account that shorter or stiffer chains have a more rodlike conformation with a lower probability of Kuhn segments making contact, thereby

reducing the excluded volume. Values of $K(N_K)$ may be obtained from tables given in ref 15.

Repulsion between charged sites causes the chain to stretch. Unlike the case of uncharged polymers, the value of L_p is not solely determined by the primary structure of the polymer backbone but is also affected by repulsion between charged sites. Hence, for polyelectrolytes the charge density on the chain and the electrolyte concentration will also affect α_{ev}. It was shown by Odijk,[17] and by Fixman and Skolnick,[18] that L_{p0} and the electrostatic contribution to the persistence length L_{pe} are additive: $L_p = L_{p0} + L_{pe}$. The electrostatic persistence length depends on the charge density of the polymer chain, which in turn is determined by the average distance L_σ between two charges along the chain. Often, the charge density is discussed in terms of a dimensionless charge density parameter λ, which is defined as the ratio L_B/L_σ, where L_B is the Bjerrum length given by

$$L_B = \frac{{q_e}^2}{4\pi\epsilon_0\epsilon_r kT} \tag{5}$$

Here, q_e represents the charge of an electron, ϵ_0 is the dielectric permittivity of vacuum, ϵ_r is the relative permittivity of the solvent, and kT has its usual meaning. In water at 298 K, L_B has a value of 0.714 nm. As will be discussed below, the presence of counterions close to the chain reduces the charge density on the chain, causing the effective charge density parameter λ_{eff} to be different from λ. In the Odijk−Skolnick−Fixman (OFS) approach,[17,18] the electrostatic persistence length L_{pe} is given in terms of the effective magnitude of the charge density parameter. Their expression for L_{pe} reads

$$L_{pe} = \frac{1}{4L_B\kappa^2}{\lambda_{eff}}^2 \tag{6}$$

where κ is the inverse Debye−Hückel screening length defined by $\kappa^2 = 2F^2c_{salt}/\epsilon_0\epsilon_r RT$ for a 1:1 electrolyte with concentration c_{salt}. In evaluating λ_{eff}, we will calculate its magnitude taking CMC as a line charge (according to Odijk[9,19]) and from the Poisson−Boltzmann equation for a uniformly charged cylinder.[8,16]

In the wormlike chain model for polyelectrolytes the excluded volume β is composed of three additive contributions: a hard-core β_c, an electrostatic contribution β_e, and an attractive β_a. Treating a Kuhn segment as a cylinder, the hard-core contribution is the excluded volume of a cylinder with radius a and length $2L_p$: $\beta_c = \pi a(2L_p)^2$.[16] The second contribution is the repulsive interaction between the charges on the chain. Fixman and Skolnick[20] derived the following expression for the electrostatic contribution β_e:

$$\beta_e = \frac{8{L_p}^2}{\kappa}R(\omega) \tag{7}$$

with ω being a parameter depending on λ_{eff}, the radius of the cylinder, and the ionic strength.[16,20] For our analyses values of $R(\omega)$ are interpolated from tabulated values given in ref 20. The third contribution, the attractive interaction between two segments, is calculated from the condition that β equals zero at the salt concentration for which Θ-conditions are reached ($-\beta_a = \beta_c + \beta_e$). For CMC the salt concentration for Θ-conditions is not known precisely. Davis estimated it at 5 mol L^{-1} NaCl. In our calculations we will use his value for β_a (-197 nm^3 [8]). The electrostatic wormlike theory will be applied to the relation between M (or equivalently L_c) and R_g as inferred from SEC−MALLS. Assuming some value for L_{p0}, R_{g0} is calculated from M by using eq 2. The electrostatic persistence length is calculated with eq 6. The chain expansion factor is a function of L_p and L_c. R_g is calculated from R_{g0} and eqs 3 and 4. At a given salt concentration L_{p0} is the only unknown parameter; it is used as a fitting parameter to match R_g, as inferred from SEC−MALLS with its calculated values.

As mentioned before, the charge density of a polyelectrolyte is affected by the presence of counterions. The charges on the chain will give rise to an electric field around the polyelectrolyte. Assuming a uniform distribution of the charged groups, a uniformly charged cylinder may serve as an adequate model for the evaluation of the local electrostatic field. This implies that the polymer backbone is supposed to be rigid on a length scale of several monomers. Within this model, the electrical potential ψ as a function of the distance from the chain can be obtained by solving the Poisson−Boltzmann (PB) equation for a charged cylinder. Besides the surface potential, the solution of the PB equation also provides the relation between λ and λ_{eff}.[16] Manning[21] derived an analytical expression for ψ by solving the PB equation in its linearized form, i.e., putting $\sinh\psi \approx \psi$. According to Manning's results $\lambda_{eff} = L_B/L_\sigma = \lambda$ for $\lambda \leq 1$. However, when L_σ becomes less than L_B ($\lambda > 1$), the effective spacing length equals L_B: counterions become very strongly localized around the polyelectrolyte, reducing λ_{eff} to 1. Without the approximation $\sinh(\psi) \approx \psi$, the PB equation cannot be solved analytically. However, its solution can be obtained numerically. As in the counterion condensation theory, numerical calculations show that λ_{eff} may be lower than λ. The dependence, however, is quite different[22,23] from that proposed by Manning. In this paper λ_{eff} was calculated numerically from the full PB equation. The numerical procedure is described in the Appendix.

Dissociation of a Polyacid in Solution. In general, the dissociation of a weak polyacid satisfies the equation

$$\mathrm{pH} = \mathrm{p}K_a + \log\left(\frac{\alpha}{1-\alpha}\right) = \mathrm{p}K_0 + \Delta\mathrm{p}K + \log\left(\frac{\alpha}{1-\alpha}\right) \tag{8}$$

where α is the fraction of dissociated acid groups (degree of ionization), pK_a is the negative logarithm of the effective (α-dependent) dissociation constant, and pK_0 is the negative logarithm of the *intrinsic* dissociation constant (pK_a at $\alpha = 0$). The ΔpK term represents the shift in the dissociation constant that is due to the change in the electrostatic free energy G_e of a polyacid upon variation in the number n of negatively charged groups:[10]

$$\Delta\mathrm{p}K = \frac{0.4343}{kT}\left(\frac{\partial G_e}{\partial n}\right)_\kappa \tag{9}$$

In the following, two models are treated which relate structural parameters to the dissociation behavior of a polyelectrolyte in aqueous solution. Both consider the

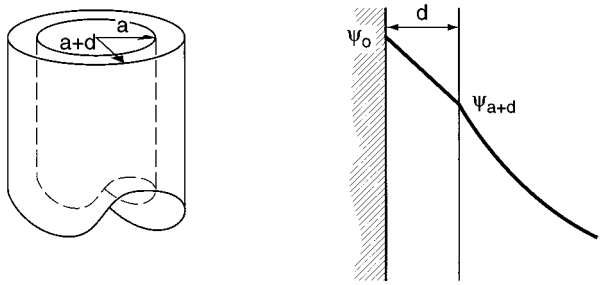

Figure 1. Schematic picture of a uniformly charged cylinder used a model for a CMC molecule on a length scale L_p.

work that is needed to displace an electrical charge (a proton) from the surface of the polyacid to a distance far from the surface. This work is directly related to the difference in electrical potential at the surface of the polymer (ψ_0) and the potential at infinity (ψ_∞). Since ψ_∞ is zero by definition, $(\partial G_e/\partial n)$ effectively equals $q_e\psi_0$. In the first model it assumed that the chain may be considered as a uniformly charged cylinder. A schematic picture of the cylindrical model is given in Figure 1. The potential difference ψ_0 can be divided into two contributions. At a given degree of dissociation the charge density of the polyacid is represented by its corresponding value of λ. In the region from a to $a + d$ the cylinder is surrounded by a Stern layer with a thickness d, which represents the distance of closest approach of ions to the polyacid surface. At distance $r > d$ the cylinder is surrounded by a diffuse double layer. The potential at $a + d$ (ψ_{a+d}) is calculated from the numerical integration of the full PB equation for a charged cylinder. Then, the potential difference over the Stern layer, the second contribution to ψ_0, is calculated from λ and the expression for the capacitance of a cylindrical capacitor. Considering CMC as a cylinder with radius a, the expression for ΔpK is[24]

$$\Delta pK = \frac{0.4343 q_e \psi_{a+d}}{kT} + \frac{0.8686 q_e{}^2 \mathrm{ds}}{4\pi\epsilon_0\epsilon_r L_b kT}\alpha \ln\left(\frac{a+d}{a}\right) \quad (10)$$

In the previous paragraph the chain is considered as a uniformly charged cylinder; i.e., the presence of discrete charges is ignored. The localization of the charges is explicitly taken into account by Katchalsky and Lifson.[11] They calculated ΔpK from the change in the electrostatic free energy that takes place upon charging an uncharged polymer. The process of charging is divided into three steps, each contributing to G_e. Charges interact by a screened Debye−Hückel potential $[\sim\exp(-\kappa r)/r]$. They are assumed to be equally spaced along the chain at a distance r. Summing up the contributions to G_e (stretching of the chain, buildup of the ionic atmosphere around charged groups, and averaging of $\exp(-\kappa r)/r$ for all pairs of interacting charges over all chain configurations), they obtained for the variation in the electrostatic free energy[11,12]

$$\left(\frac{\partial G_e}{\partial n}\right)_\kappa = \frac{2n q_e{}^2}{4\pi\epsilon_0\epsilon_r h}\left[\ln(1+x) - \alpha\frac{(k_i - k_0)}{2k}\frac{x}{1+x}\right]$$

$$x = \frac{6h}{\kappa h_0{}^2} \quad (11)$$

In eq 11, h_0 and h represent the end-to-end distance of the uncharged polymer and the chain carrying n charges, respectively. The number of monomers in a Kuhn segment is denoted by k. For the uncharged chain, $k = k_0$. Charging the chain will increase the number of monomers per Kuhn segment eventually to k_i (the number of monomers in a Kuhn segment when the chain is fully dissociated). It is assumed that k is a linear function of α: $(1 - \alpha)k_0 + \alpha k_i$. Katchalsky and Lifson choose for h_0 the expression of the unperturbed end-to-end distance of a Gaussian coil. In their discussion about the choice for h, they state that the expression for a fully stretched molecule is applicable. In our opinion it is more realistic to consider the charged chain also as a random coil. Equation 11 can be used as the starting point for the determination of the intrinsic persistence length of a polyelectrolyte.

Let the number of monomeric units in the chain be denoted by Z, then the number of charges on a CMC molecule equals $n = \alpha Z\mathrm{ds}$. As we assume a Gaussian coil conformation for both the uncharged and the charged molecule, the expressions for the mean square of the end-to-end distances are represented by $h_0{}^2 = Zk_0b^2$ and $h^2 = Zkb^2$, respectively, where b is the length of a monomer (0.515 nm[26]). In the model of Katchalsky and Lifson excluded volume effects are not taken into account. The increase in the coil dimension, i.e., the swelling of the chain, is accounted for by increasing the number of monomers in a Kuhn segment from k_0 to k. Upon inserting these expressions for h_0 and h into eq 11, an expression is obtained that contains a chain length dependence. In the limit of long chains ($Z \rightarrow \infty$) the Z dependence vanishes. Realizing that the ratio $(k - k_0)/k$ equals L_{pe}/L_p and $k_0b = L_{K0} = 2L_{p0}$ for a long wormlike chain, combination of eq 11 with eqs 8 and 9 yields

$$\mathrm{pH} = pK_0 + \log\left(\frac{\alpha}{1-\alpha}\right) + \frac{0.4343}{kT}\frac{12 q_e{}^2 \mathrm{ds}}{4\pi\epsilon_0\epsilon_r\kappa 2L_{p0}b}\alpha\left(1 - \frac{1}{2}\frac{L_{pe}}{L_{p0} + L_{pe}}\right) \quad (12)$$

where we have used only the first term in the Taylor expansions for $\ln(1 + ax)$ and $ax/(1 + ax)$, which amounts to ax for both. The above equation offers the possibility of deducing the intrinsic persistence length from titration experiments.

Experimental Section

Materials. Carboxymethyl cellulose was prepared by Akzo Nobel by reaction of cellulose (cotton linters), NaOH, and sodium monochloroacetate ($ClCH_2COONa$). During the reaction, hydrogen atoms at the glucose hydroxyl groups are substituted by CH_2COONa. The average number of substituents per glucose monomer is denoted as the degree of substitution (ds). In this way CMCs were prepared with ds = 0.75, 0.91, 0.99, and 1.25, respectively; these samples will be denoted hereafter as samples 1. Subsequently, portions of these samples were treated with H_2O_2 in ethanolic slurry to cause random cleavage between glucose units, thereby reducing the molar mass. Adding different amounts of H_2O_2 yielded series with decreasing chain length (samples 2−5). In this way a set of 20 CMCs was prepared, varying in degree of substitution and chain length (see Table 1).

In Figure 2 the structure of CMC is given schematically. The monomeric unit of the CMC backbone consists of D-glucose residues linked through β-1,4 bonds. Depending on whether the hydroxyl groups in a glucose unit are un-, mono-, di-, or trisubstituted, CMC molecules can in principle consist of eight different monomers. The composition of the CMC samples was

Table 1. Average Molar Masses M_w and M_n, Polydispersity Index M_w/M_n, and Radius of Gyration R_g of (Depolymerized) CMC Samples with Different Degrees of Substitution[a]

ds	sample no.	M_n (kg mol^{-1})	M_w (kg mol^{-1})	M_w/M_n	R_g (nm)
0.75	1	520	1100	2.2	140
	2	310	740	2.4	100
	3	200	400	2.0	75
	4	85	190	2.2	40
	5	45	120	2.7	30
0.91	1	510	1100	2.2	140
	2	470	880	1.9	120
	3	170	340	2.0	55
	4	100	210	2.1	40
0.99	1	570	1200	2.0	160
	2	390	640	1.6	95
	3	80	180	2.3	35
1.25	1	370	1100	2.9	130
	2	330	660	2.0	90
	3	200	380	1.9	50
	4	120	210	1.8	30

[a] Samples indicated by number 1 were not depolymerized. Numbers 2−5 refer to samples that were depolymerized (by H_2O_2) to an increasing extent. Due to the low light scattering intensity, characterization of some depolymerized samples could not be carried out.

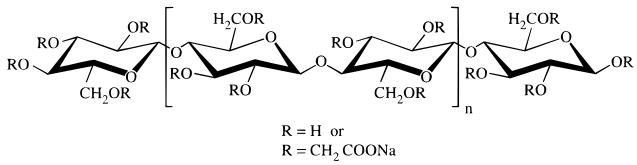

Figure 2. Repeating unit of carboxymethyl cellulose. The D-glucose units are linked through β-1,4 bonds. R represents a hydrogen atom (unsubstituted hydroxyl group) or a CH_2-COONa group (substituted hydroxyl group).

analyzed after acidic hydrolysis by HPLC and quantified from the refractive index by taking the peak height surface area in a 100% analysis, yielding consistent and accurate data.

SEC−MALLS. CMC solutions were prepared in the following way. First, CMC was dissolved in demineralized water. While dissolving, the samples were gently shaken for 16 h at room temperature. Then sodium nitrate solution was added to obtain an electrolyte concentration of 0.02 or 0.1 mol L^{-1}. In potentiometric titrations NaCl was used as the electrolyte, but as NaCl damages the SEC equipment, $NaNO_3$ was used as the electrolyte for SEC. The addition of salt was carried out after dissolution in order to minimize the presence of aggregated, not fully dissolved, CMC. It was found that when CMC was dissolved in the presence of salt, the solution contained "scaly" particles, which is an indication that CMC was not dissolved completely. The presence of these particles was more pronounced at high salt concentrations.

The concentration of the polymer solutions was chosen such that the overlap concentration was not exceeded, but it was large enough to obtain a measurable light scattering intensity. The following concentrations were used: 1000, 1000, 1500, 2000, and 2500 mg L^{-1} for samples 1−5, respectively. Prior to the SEC measurements the samples were filtered over a 0.45 μm hydrophilic Durapore (Millipore) membrane.

The samples were eluted at pH = 7 on a set of three columns (G6000 PW, G5000 PW, and G3000 PW) with a flow rate of about 0.95 mL min^{-1}. No adsorption on the columns was observed (i.e., all injected polymer was eluted from the columns). A DAWN-DSP-F (Wyatt Technology Co.) MALLS detector was used to obtain on-line determination of the absolute molar mass and the radius of gyration of each fraction eluting. The light scattering signal was detected simultaneously at eleven scattering angles θ, ranging from 44 to 151°. After the scattering intensity was converted into a Raleigh ratio R, the quantity Kc/R was plotted against $\sin^2(\theta/2)$ (Zimm plot[25]). In Kc/R, c is the CMC concentration and K is an optical constant given by $4\pi^2 n_D^2(\partial n_D/\partial c)^2/\lambda_0^2 N_{AV}$, where λ_0 is the wavelength of the He−Ne laser, n_D is the refractive index of the solvent, and $\partial n_D/\partial c$ is the refractive index increment of CMC in aqueous solution. For each fraction, M and R_g were determined from the intercept and initial slope of the Zimm plot. The CMC concentration in eluted fractions was small enough for extrapolation to zero concentration to be of no concern. Both SEC and MALLS detection were carried out at 298 K.

Determination of the concentration was performed with an interferometric refractive index detector (Optilab Wyatt Technology Co). The refractive index increment ($\partial n_D/\partial c$) at a wavelength of 632.8 nm was established at 0.163 mL g^{-1}. The value of the refractive index increment did not depend on either ds or on M_w.

Potentiometric Titrations. Sample preparation for titration experiments was nearly identical to the procedure in the SEC experiments. After CMC was dissolved, NaCl solution was added to obtain an electrolyte concentration in the range 0.01−1 mol L^{-1}. The polymer concentration was 1000 mg L^{-1} in all titration experiments. Initially, the solution pH was set to pH = 3 by addition of 0.1 mol L^{-1} HCl. Flushing with purified nitrogen was used to remove any carbon dioxide from the solutions. Titrations to pH = 11 (by addition of carbonate-free 0.1 mol L^{-1} KOH) and back-titrations to pH = 3 were carried out in an atmosphere of purified nitrogen. For pH readings a glass electrode was used. The electrode was calibrated at 298 K against nine buffer solutions in the pH range 3−11.

Titrations were performed at 298 K using a Schott Titronic T200 autoburet. The dosage of titrant was calculated on the basis of the change in pH according to previous additions. The minimum dosage volume was 0.01 mL; at the most, 0.5 mL of titrant was added. After addition of titrant, pH readings (accuracy of 0.001 pH units) were carried out. When the change in pH after addition was less than 0.01 pH unit per minute, new titrant was added. In general the time between two additions was about 5 min.

The proton release (forward titration with KOH) or take up (backward titration with HCl) by the polyelectrolyte were calculated from the dosage and the pH change due to the addition of titrant. The relation between the activity, calculated from the pH, and the concentration of free protons or hydroxyl ions was established through titration of HCl solution with the same electrolyte concentration as in the polyelectrolyte titration. The degree of ionization (α) in the forward titration was calculated as

$$\alpha = \frac{c_p V\mathrm{ds} - (n_{max} - n_r)}{c_p V\mathrm{ds}} \qquad (13)$$

where n_r is the amount of protons released from the polyelectrolyte, n_{max} is the maximum release of protons, c_p is the monomer concentration, and V is the volume in which the polyelectrolyte was dissolved. The value of n_{max} is identified as the point where the release of protons is zero; i.e., addition of base only leads to a change in pH. In the case of the back-titration α is calculated from the proton uptake n_u by the polyelectrolyte: $\alpha = 1 - n_u/(c_p V\mathrm{ds})$.

Results and Discussion

CMC Monomer Composition. The monomer composition of the samples as obtained from HPLC analysis is presented in Figure 3. Spurlin[26] proposed a model from which the monomer composition of a sample with known ds can be calculated. In this model a relative rate constant is assigned to each of the hydroxyl groups at the 2-, 3-, or 6-position. It is assumed that substitution reaction occurs at random (i.e., all hydroxyl groups are equally accessible during the reaction) and that

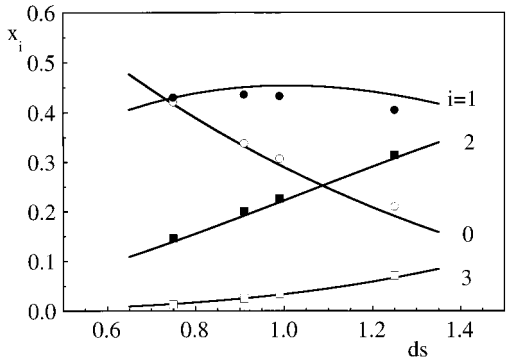

Figure 3. Composition of CMC samples by mole fraction (x_i) of substituted monomers. Numbers indicate the number of substituted hydroxyl groups per monomeric unit: $i = 0$ (○) unsubstituted glucose unit, and $i = 1$ (●) mono-, $i = 2$ (■) di-, and $i = 3$ (□) trisubstituted glucose. Solid curves refer to calculated mole fractions corresponding to a random distribution of the substituents. Compositions relate to samples 1. Identical results were obtained for the depolymerized samples.

relative reactivities of the three hydroxyl groups do not change with ds. Furthermore, it is assumed that the rate of the substitution reaction is first order in the concentration of the hydroxyl groups. Calculated mole fractions based on Spurlin's statistical model are also included in Figure 3 (solid curves). Mole fractions are calculated using the relative reaction rate constants that Reuben et al.[27] obtained from the monomer composition of a series of CMC samples having ds ranging from 0.55 to 2.17. Their calculated reaction rate constants were in good agreement with data reported in the literature (see for instance Buytenhuys and Bonn[28]). Therefore we assume that their data relate to a random distribution of the substituents along the polymer chain. Ma et al.[29] determined for CMC ranging in ds from 0.51 to 1.55 the average number monomers that are present in blocks consisting of either substituted or unsubstituted glucose units by means of enzymatic cleavage. From their analysis they conclude that the crystalline structure of cellulose is almost completely absent in CMC and that substitution of glucose units takes place at random. Their analysis reveals that the average number of unsubstituted glucose units ranges from 3.4 to 1.8 monomeric units for ds = 0.51 and 1.55, respectively. With respect to the monomeric composition the analysis in ref 29 only yields information about the mole fraction of unsubstituted glucose units. In correspondence with random substitution, good agreement was found with Reuben for the amount of unsubstituted glucose. As can be seen from Figure 3, the agreement between the monomer composition based on a random distribution of substituents and the composition of our samples is good. On the basis of this agreement, we conclude that in our samples the substituents are also randomly distributed over the polymer chain and that the number of long unsubstituted regions is negligible.

SEC−MALLS. In Figure 4 some typical results for the molar mass distribution as obtained from SEC−MALLS measurements are given. The figure shows the differential molar mass distribution (DMMD) for CMC samples 1 and 4 with ds = 0.91 determined in 0.02 and 0.1 mol L^{-1} $NaNO_3$ solution, respectively. The molar mass distribution given in Figure 4a is determined using a linear extrapolation of the scattered intensity to zero angle. Figure 4b shows the result when a nonlinear extrapolation (second-order polynomial) is used. DMMD is determined by differentiation of the

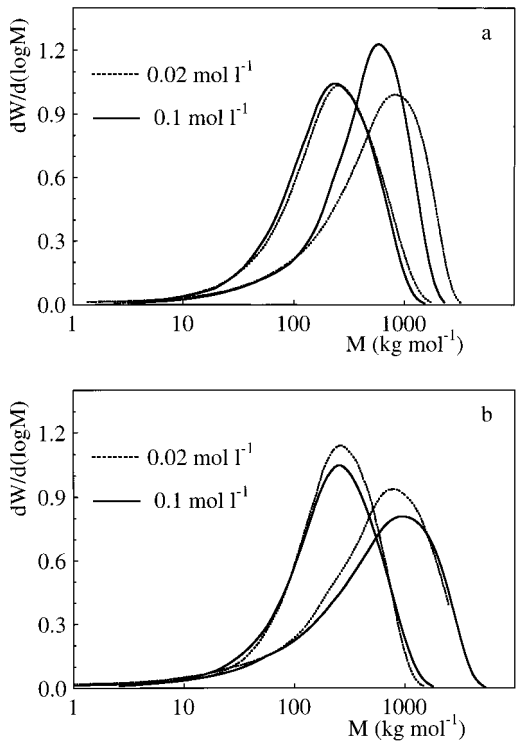

Figure 4. Molar mass distribution of two CMC samples (ds = 0.91) M_w = 1100 and 210 kg mol^{-1}. Distributions were determined in solutions containing 0.02 or 0.1 mol L^{-1} $NaNO_3$ (indicated in figure). Distributions were obtained (a) by using a linear Zimm plot or (b) by using a quadratic extrapolation to zero scattering angle.

cumulative mass fraction $W(M)$ (i.e., the mass fraction of molecules having a molecular mass less than M) with respect to the logarithm of M.[30] For a detailed description of the DMMD calculation from SEC data, the reader is referred to Shortt.[30] As the chain charge density, and accordingly ds, affects the size of polyelectrolytes, a distribution of ds within a sample would influence the fractionation. However, since all CMC samples were prepared under well-defined experimental conditions, probably the distribution in ds is negligible. Comparing the molar mass distributions for the high M sample (sample 1) as obtained at different electrolyte concentrations, it can be seen that the distribution depends significantly on the method of extrapolation to zero scattering angle. As can be seen from Figure 4a, the distribution for sample 1 is shifted to higher M at 0.02 mol L^{-1} $NaNO_3$ if a linear extrapolation is used. Since the distribution is an intrinsic property of a sample, it is not likely to depend on the electrolyte concentration. It might be supposed that a high electrolyte concentration leads to some aggregation of CMC. If the chains contain long regions of unsubstituted or slightly substituted monomers, screening of the few charges allows the formation of H-bridges between those regions, which may lead to formation of aggregates. Since aggregates have a higher molar mass, their presence will shift the distribution to higher M compared to an unaggregated solution (i.e., a solution containing less electrolyte). However, the experiments show the opposite trend, indicating that the lack of coincidence of distributions in 0.02 and 0.1 mol L^{-1} $NaNO_3$ is probably not caused by the presence of aggregates. Upon using a nonlinear extrapolation method, both distributions of the low and high M sample are shifted to higher molar mass. The position of the peak in the DMMD now gives better

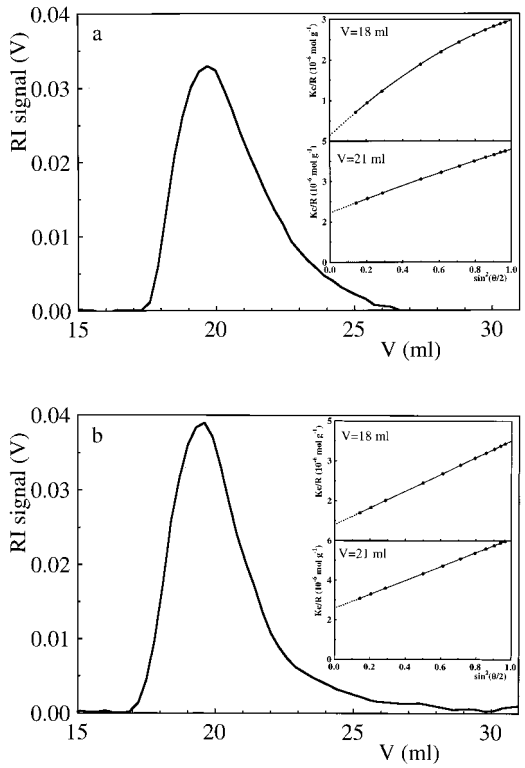

Figure 5. Elution chromatogram of CMC ds = 0.91 (sample 1) as obtained in (a) 0.1 mol L^{-1} $NaNO_3$ and (b) 0.02 mol L^{-1} $NaNO_3$. The insets show Zimm plots at two elution volumes (indicated in figures). The molar mass of an eluted fraction decreases with increasing elution volume.

agreement between distributions obtained in 0.02 and 0.1 mol L^{-1} $NaNO_3$. Though better agreement is found between the distributions, a discrepancy still exists between those obtained at low and at high salt concentrations. Complete treatment of the data requires a statistical treatment (F-test[31]) of the Zimm plot of each eluted fraction to decide which extrapolation method (linear or nonlinear) should be used. Unfortunately, our setup does not provide for such a treatment. We used the position of the peak as the criterion to decide which extrapolation method is suitable for our data treatment. The other nondepolymerized CMC samples as well as the depolymerized fractions 2 and 3 show the same behavior as presented in Figure 4. Measurements on samples 4 and 5 (ds = 0.75, 0.99, and 1.25) were not carried out in 0.02 mol L^{-1} $NaNO_3$.

The lack of coincidence of the molar mass distributions is caused by a downward curvature in Kc/R at low angles ($\theta < 75°$). The downward curvature is illustrated by Figure 5, where we give the concentration (measured by the index of refraction) of eluted fractions (CMC ds = 0.91, sample 1) as a function of the elution volume. Insets show Zimm plots at different volumes in the chromatograms. As can be seen, nonlinearity is observed in 0.1 as well as in 0.02 mol L^{-1} $NaNO_3$, the effect being most pronounced in 0.1 mol L^{-1} $NaNO_3$ for CMC of high M. As the molar mass is obtained from the intercept of a Zimm plot (i.e., extrapolation of Kc/R to zero scattering angle), the magnitude of M is rather sensitive to the extrapolation method. The origin of the nonlinear Zimm plots is not clear. As we stated in the previous paragraph, the presence of aggregated CMC is not likely the cause of the nonlinearity. We will touch upon this in the following paragraphs. It was already pointed out by Mijnlieff et al.[32] that the use of a linear extrapolation may lead to errors in the determination of the molar mass of a polymer sample from static light scattering.

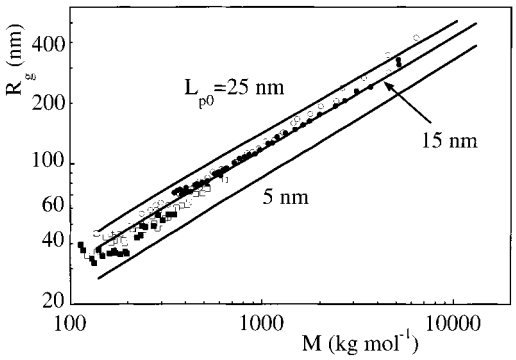

Figure 6. Relation between the radius of gyration R_g and molar mass M for CMC ds = 0.91 SEC fractions. Samples with different degrees of polymerization are indicated by different symbols: (○) samples 1, (●) 2, (□) 3, (■) 4. Solid curves refer to calculations using the wormlike chain model.[8] Different values for intrinsic persistence length L_{p0} are indicated.

From Figure 4 it can also be seen that the molar mass distribution is quite narrow, almost as narrow as in condensation polymers. The polydispersity is represented by the ratio M_w/M_n (Table 1), where M_w and M_n are the weight and number molar mass averages, respectively. The polydispersity ratio for the nondepolymerized samples (about 2.5) is comparable to M_w/M_n for cotton linters cellulose, which is about 2.2,[33] but is substantially lower as compared to the majority of commercial CMC types derived from wood cellulose, which show polydispersities from 6 to even 20. All results refer to experiments carried out in 0.1 mol L^{-1} $NaNO_3$. The molar mass of the nondepolymerized samples does not vary significantly with ds. As CMC samples with different ds were prepared from the same starting material, samples 1 do not differ much in average molar mass.

For CMC samples 1 to 4 with ds = 0.91, but differing in average molar mass, the relation between radius of gyration and molar mass in 0.1 mol L^{-1} $NaNO_3$ is represented in Figure 6. Both M and R_g were determined by using the nonlinear extrapolation. For samples 5 the intensity of the scattered light was too low, so that characterization could not be carried out accurately. Owing to the small proportions of the scattering molecules the low scattered intensity exhibited a high noise level. The samples supplement each other rather satisfactorily. Similar observations where made for samples with other ds. The full curves in the figure represent the relation between R_g and M calculated according to the wormlike chain model.[8] The relation was calculated using different values for the intrinsic persistence length. As can be seen from this figure, the value of L_{p0} lies in the range 15−25 nm.

A graph similar to Figure 6 is presented in Figure 7. In this figure the radius of gyration is given as a function of the number of Kuhn segments, N_K ($=L_c/2L_p$), for CMC ds = 0.75 and ds = 1.25. The two upper figures relate to CMC samples 1−5 in 0.1 mol L^{-1} $NaNO_3$, the lower to CMC samples 1−3 in 0.02 mol L^{-1} $NaNO_3$. The relation between R_g and N_K calculated with the wormlike chain theory according to Davis is represented by the solid curves. Best fits to the experimental data were obtained when L_{p0} was set to 17 nm (0.02 mol L^{-1} $NaNO_3$) or 15 nm (0.1 mol L^{-1}), irrespective of ds. A

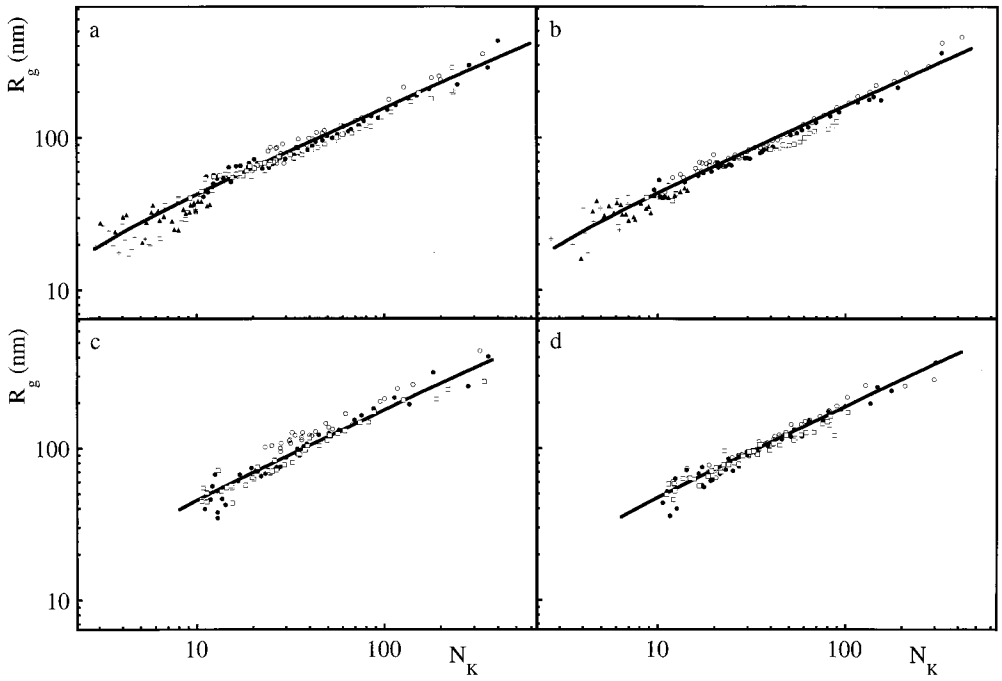

Figure 7. Relation between number of Kuhn segments N_K and radius of gyration R_g for CMC in a 1:1 electrolyte solution: (a) CMC ds = 0.75 in 0.1 mol L^{-1} $NaNO_3$; (b) ds = 1.25 in 0.1 mol L^{-1} $NaNO_3$; (c) ds = 0.75 in 0.02 mol L^{-1} $NaNO_3$; (d) ds = 1.25 in 0.02 mol L^{-1} $NaNO_3$. Samples with different degrees of polymerization are indicated by different symbols: (○) samples 1, (●) 2, (□) 3, (▲) 4, (+) 5. The solid curves were calculated according to the wormlike chain model[8] using L_{p0} = 17 nm for 0.02 mol L^{-1} $NaNO_3$ and L_{p0} = 15 nm for 0.1 mol L^{-1} electrolyte, respectively.

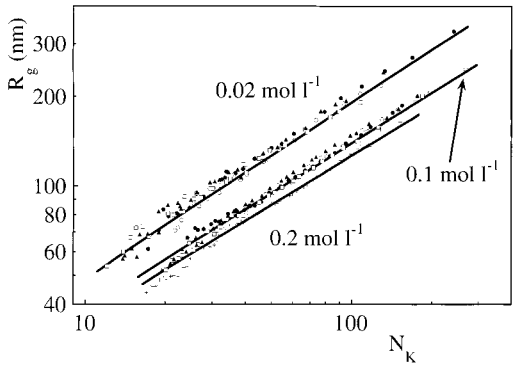

Figure 8. Relation between number of Kuhn segments (N_K) and radius of gyration (R_g) for CMC in a 1:1 electrolyte solution (indicated in figure). Different symbols refer to samples 2 differing in ds: (○) ds = 0.75, (●) ds = 0.91, (□) ds = 0.99, and (▲) ds = 1.25 and (+) sample 1 ds = 0.91. The solid curves were calculated according to the wormlike chain model[8] using L_{p0} = 17 nm for 0.02 mol L^{-1} $NaNO_3$ and L_{p0} = 15 nm for 0.1 and 0.2 mol L^{-1} electrolyte, respectively. For the treatment of sample 1 in 0.2 mol L^{-1} $NaNO_3$, see text.

linear relation between log N_K and log R_g is observed in 0.1 mol L^{-1} $NaNO_3$ for $N_K > 10$, indicating a random coil conformation of the polymer. For $N_K < 10$ the local rodlike character of the chain shows up from a slight downward bending of the curves. In 0.02 mol L^{-1} $NaNO_3$ the downward bending is observed for $N_K < 20$, illustrating that the local stiffness of the chain increases with decreasing salt concentration. The increase of L_p with decreasing salt concentration also shows up from the dependence of R_g on the concentration $NaNO_3$. In 0.02 mol L^{-1} $NaNO_3$, R_g is found to be larger than in 0.1 mol L^{-1} $NaNO_3$. The electrolyte dependence of R_g can be deduced from Figure 7, it is shown more clearly in Figure 8. In Figure 8 the relation between R_g and N_K is shown for CMC samples 2 with ds from 0.75 to 1.25 for two electrolyte concentrations. The lower curve (0.2 mol L^{-1} electrolyte) refers to CMC sample 1 (ds = 0.91). The solution preparation of this sample was somewhat different from previous preparations. After dissolution in demineralized water, KOH solution was added to a concentration of 0.1 mol L^{-1}. After 15 h the sample was brought to pH = 7 with HNO_3, yielding a total $NaNO_3$ concentration of 0.2 mol L^{-1}. This treatment, carried out in a nitrogen atmosphere, was applied because in a highly basic medium hydroxyl groups are dissociated. The dissociation disrupts any hydrogen bonds between cellulose chains, the bond-breaking process being enhanced by the repulsion between charged groups. Thus, in a basic medium the presence of aggregated CMC is unlikely. The linear region in the relation between the radius of gyration and molar mass often obeys the scaling law $R_g \sim M^\nu \sim N_K^\nu$. The exponent ν contains information about structural properties of a macromolecule (e.g., if a chain is a random coil or is branched) and the solvent quality.[34,35] Schulz and Burchard[35] determined ν for CMC in 0.1 mol L^{-1} NaCl by viscometry and found $\nu = 0.28$. From this low number and determination of the hydrodynamic radius they concluded that their solutions contained a considerable amount of aggregated CMC. In 0.1 mol L^{-1} KOH we obtain $\nu = 0.59$, which indicates that in KOH CMC may be considered as a linear polymer in a good solvent.[34,35] As ν is rather sensitive to the presence of aggregates,[35] we conclude that in 0.1 mol L^{-1} KOH no (or very little) aggregated CMC is present. The value $\nu = 0.59$ is preserved in the $NaNO_3$ solutions. Hence, measurements carried out in 0.1 mol L^{-1} KOH yield results similar to those in 0.1 mol L^{-1} $NaNO_3$, albeit that the sample is somewhat degraded (depolymerized) due to presence of oxygen in the alkaline solution. The agreement between ν in KOH and in $NaNO_3$ indicates that aggregated CMC can be present in our samples, only in very small amounts. Cryotransmission electron microscopy supports this conclusion.

Table 2. Electrostatic Excluded Volume β_e, Expansion Factor α_{ev}, and Electrostatic Persistence Length L_{pe} Calculated for CMC with ds = 0.75 According to the Models of Odijk[9] and Davis[8,a]

c_{NaCl} (mol L^{-1})	N_K	$K(N_K)$	β_e (nm^3)		α_{ev}		L_{pe} (nm)	
			Odijk	Davis	Odijk	Davis	Odijk	Davis
0.02	20	0.839	10700	8000	1.237	1.141	1.62	1.37
0.02	100	1.171	10700	8000	1.293	1.297	1.62	1.37
0.02	200	1.223	10700	8000	1.455	1.370	1.62	1.37
0.10	20	0.839	3100	1900	1.156	1.053	0.32	0.31
0.10	100	1.171	3100	1900	1.198	1.132	0.32	0.31
0.10	200	1.223	3100	1900	1.324	1.224	0.32	0.31

[a] The intrinsic persistence length is set at 13 nm. In Odijk's approach $K(N_K)$ has a constant value of 1.33.

Table 3. Electrostatic Excluded Volume β_e, Expansion Factor α_{ev}, and Electrostatic Persistence Length L_{pe} Calculated for CMC with ds = 1.25 According to the Models of Odijk[9] and Davis[8,a]

c_{NaCl} (mol L^{-1})	N_K	$K(N_K)$	β_e (nm^3)		α_{ev}		L_{pe} (nm)	
			Odijk	Davis	Odijk	Davis	Odijk	Davis
0.02	20	0.839	10700	12200	1.237	1.157	1.62	2.93
0.02	100	1.171	10700	12200	1.293	1.323	1.62	2.93
0.02	200	1.223	10700	12200	1.455	1.401	1.62	2.93
0.10	20	0.839	3100	2900	1.156	1.073	0.32	0.77
0.10	100	1.171	3100	2900	1.198	1.173	0.32	0.77
0.10	200	1.223	3100	2900	1.324	1.144	0.32	0.77

[a] The intrinsic persistence length is set at 13 nm. In Odijk's approach $K(N_K)$ has a constant value of 1.33.

As can be seen from Figure 8, the degree of substitution does not affect the relation between R_g and N_K. This is found in 0.1 as well as in 0.02 mol L^{-1} $NaNO_3$. According to Odijk, the lack of dependence on ds indicates that at pH = 7, CMC is above the threshold for the onset of counterion condensation. At pH = 7, CMC is fully dissociated. Indeed, the value of the effective charge parameter λ exceeds the limiting value 1 for a fully dissociated CMC sample with ds = 0.75 (λ = ds L_B/L_{mon} = 1.04, if L_{mon} = 0.52 nm[26] is substituted for the monomeric length of a glucose unit). Since the other samples have even higher charge densities, they will also exceed the limiting value. In evaluating R_g versus N_K, we used the wormlike chain model as presented by Davis.[8] Therefore, in the calculation of λ_{eff} we used the model of the uniformly charged cylinder rather than putting λ_{eff} = 1 for all experiments. The calculated relation between R_g and N_K for the three electrolyte concentrations is represented by the solid curves. As will be shown in the discussion regarding the potentiometric titrations, the cross-section of the cylinder shows a dependence on the degree of substitution. Taking into account this ds dependence, the calculated relation between R_g and N_K shows only a slight dependence on the degree of substitution. For this reason, in Figure 8 only the calculated curve for ds = 0.91 is shown. Any dependence on ds is too weak to be deduced from our experimental data. Qualitatively, both Davis's and Odijk's approaches give good agreement with experimental results. Best fits to the experimental data were obtained using Davis's approach when L_{p0} was set to 17 nm (0.02 mol L^{-1} $NaNO_3$) or 15 nm (0.1 and 0.2 mol L^{-1}). The bare persistence length using the Odijk model is lower than that obtained by the Davis model. Using Odijk's approach we obtain 13 nm (0.02 mol L^{-1} $NaNO_3$) and 11 nm (0.1 and 0.2 mol L^{-1} $NaNO_3$), respectively.

Why do the models of Odijk and Davis give different quantitative results? As stated before, in Odijk's approach the function $K(N_K)$ in eq 4 is assumed to have a fixed value of $^4/_3$, which is valid for chains consisting of many (infinite number of) Kuhn segments. For our samples with the highest molar mass, this assumption is reasonable. For L_p = 15 nm (L_K = 30 nm) the number of Kuhn segments for CMC with L_c = 10 000 nm equals 330 and $K(N_K)$ reaches the value of about 1.2.[16] Thus, for the highest molar mass fraction the error in Odijk's assumption is small. However for L_c = 600 nm, which covers the range of the smallest molecules, $K(N_K)$ reaches a value of only about 0.8. Consequently, putting $K(N_K)$ equal to the limiting value is only valid for a fraction of our samples. With $K(N_K) = {}^4/_3$, z is overestimated, yielding a higher number for the expansion factor. Furthermore, the assumption that a CMC molecule may be considered as a line charge tends to overestimate the electrical contribution to the excluded volume. This can be demonstrated as follows. The parameter ω in eq 7 reads[16]

$$\omega = \frac{2\pi}{L_B\kappa}\left(\frac{\lambda_{eff}}{a\kappa K_1(a\kappa)}\right)^2 e^{-2a\kappa} \tag{14}$$

with K_1 a modified Bessel function of the second kind of order one. For values $\omega > 5$ in eq 7, $R(\omega)$ may be approximated by $\pi/4(\ln(\omega) + \ln(2) + \gamma - {}^1/_2)$. Inserting $\ln(\omega)$ into the expression for $R(\omega)$ and putting $a\kappa$ equal to zero, Odijk obtains the following expression for the electrostatic excluded volume:

$$\beta_e = 2\pi L_p{}^2\frac{1}{\kappa}\left(-\ln(L_B\kappa) + \ln(\lambda_{eff}{}^2) + \ln(4\pi) + \gamma - \frac{1}{2}\right) \tag{15}$$

where γ is Euler's constant (0.577 22). The expression between brackets divided by κ, is Odijk's effective diameter of a Kuhn segment.[9] To evaluate the consequences of setting $a\kappa$ to zero and taking $K(N_K) = {}^4/_3$, we have calculated the expansion factor α for different situations, i.e., different chain lengths and ds values, at two different salt concentrations, using both Odijk's and Davis's approach. The results are presented in Tables 2 and 3. The data illustrate that the assumption of setting $K(N_K)$ at 1.33 is not legitimate for the whole range of the CMC samples. Comparing the electrostatic excluded volume according to the two models, it can be seen that Odijk's approach in general gives a higher number than Davis's. The origin for this difference lies

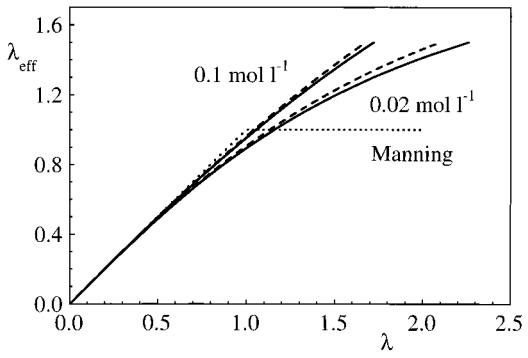

Figure 9. Effective charge parameter λ_{eff} as a function of the charge parameter λ. The curves were calculated from the numerical solution of the Poisson−Boltzmann equation for a charged cylinder. The dashed curves refer to a cylinder with radius 0.95 nm; the solid curves, to one with radius 1.15 nm. The relation according to Manning's counterion condensation theory is also included (dotted curve).

in the fact that in Odijk's expression for $\ln(\omega)$ all terms including $a\kappa$ are omitted. It can be shown that the sum of these terms has a negative value, so Davis arrives at a lower value for $R(\omega)$ than does Odijk.

The magnitude of β_e is also determined by the magnitude of L_p (see eq 7), which in turn depends on λ_{eff} (eq 6). In Figure 9 the relation between λ_{eff} and the bare charge density λ is given for two salt concentrations (0.02 and 0.1 mol L^{-1}) and two CMC radii (0.95 and 1.15 nm). These radii correspond, as will be elucidated in the following section, to CMC with ds = 0.75 and 1.25, respectively. The relation according to Manning's counterion condensation theory is also included (dotted line). If fully dissociated, CMC with ds values of 0.75 and 1.25 corresponds to $\lambda = 1.1$ and 1.7, respectively. At $\lambda = 1.1$ the difference between λ_{eff} according to Manning and λ_{eff} as obtained from the solution of the full PB equation is rather small, consequently L_{pe} according to Odijk and Davis is comparable (see Table 2). As in Odijk's approach the line charge approximation tends to overestimate β_e, its value for CMC ds = 0.75 calculated according to Davis will be lower as compared to Odijk's approach. In the case of CMC ds = 1.25 ($\lambda = 1.7$) λ_{eff} is higher when calculated from the PB equation, thereby increasing the value of β_e compared to CMC ds = 0.75. So for CMC ds = 1.25 the difference in β_e between both approaches is less than for CMC ds = 0.75. As shown in Table 3, β_e according to Davis may even exceed β_e as obtained by Odijk. In the evaluation of our data we used L_{p0} as an adjustable parameter, L_{p0} was not determined in an absolute manner (e.g., by neutron scattering). Therefore we cannot judge on basis of the outcome of our analysis which approach (Davis's or Odijks) is most suitable to determine L_{p0} from the relation between R_g and M. With respect to electrostatics, differences between Davis and Odijk will show up when $\lambda > 1$ (see Figure 9). So, the electrostatic persistence length of chains having a low charge density can be described adequately according to Odijk (see, for instance, de Nooy et al.[36]). As the Davis model gives a more complete description of electrostatics and takes molecular properties (such as chain length and cross-section of the molecule) into account, we prefer to use Davis's approach for highly charged polyelectrolytes.

Potentiometric Titrations. In Figure 10 the dissociation behavior of CMC in aqueous solution is given as a function of electrolyte concentration and ds. The curves refer to experiments that were carried out with

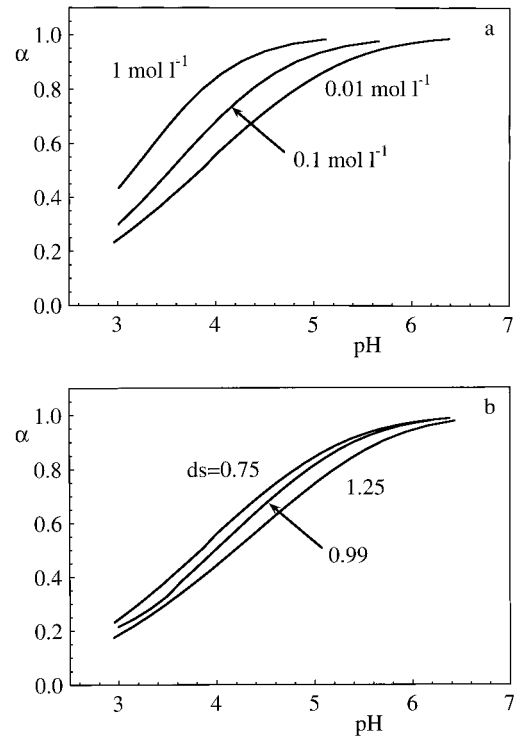

Figure 10. pH dependence of degree of dissociation (α) of CMC in aqueous solution: (a) dependence on the electrolyte concentration (NaCl) for CMC ds = 0.75; (b) dependence on ds at fixed electrolyte concentration (0.01 mol L^{-1} NaCl).

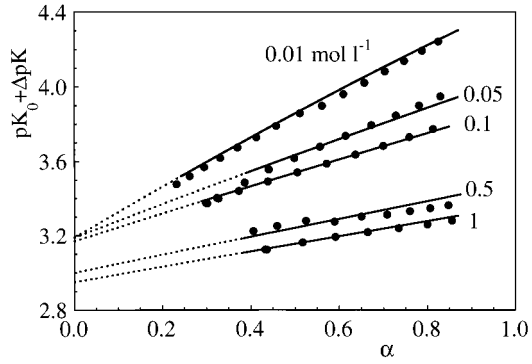

Figure 11. Apparent dissociation constant ($pK_a = pK_0 + \Delta pK$) for CMC ds = 0.75 as a function of the degree of dissociation α at various NaCl concentrations (indicated in figure). The solid curves were calculated from the numerical solution of the Poisson−Boltzmann equation for a charged cylinder (radius 0.95 nm).

sample 1. Titrations with depolymerized CMCs (up to sample 5) yield identical results; i.e., no dependence on the molar mass has been observed. As can be seen, the dissociation behavior clearly exhibits polyelectrolyte character. As an increasing number of carboxylic groups becomes dissociated, the increased charge on the chain will hamper subsequent dissociation of nondissociated groups. Salt screens the charges, thereby facilitating the dissociation, which results in a higher degree of dissociation at a given pH. As the dissociation is affected by the charge density, the dissociation constant (and thereby pK_a) will not be a constant but will depend on α. This dependence is demonstrated in Figure 11 for CMC (ds = 0.75) at various NaCl concentrations. As expected, pK_a is not constant but increases with charge density. The polyelectrolyte character is most pronounced at low salt concentrations but is still noticeable at high concentration (1 mol L^{-1}).

Table 4. Intrinsic Dissociation Constant pK_0 for CMC in Solutions with Different NaCl Concentrations[a]

ds	radius (nm)	electrolyte concentration (mol L^{-1}) 0.01	0.05	0.1	0.5	1
0.75	0.95	3.22	3.22	3.20	3.00	2.95
0.91	1.00	3.18	3.20	3.20	3.00	2.94
0.99	1.05	3.15	3.22	3.18	3.00	2.95
1.25	1.15	3.23	3.30	3.20	3.10	2.95

[a] The radii of the chain and pK_0 were obtained by fitting experimental data to the model of a uniformly charged cylinder.

The solid curves refer to pK_a as calculated from the uniformly charged cylinder model (eq 10). In all calculations, the radius of a solvated Na^+ ion (0.25 nm[37,40]) was chosen for the thickness of the Stern layer. Best fits to the experimental data were obtained using a cylinder radius of 0.95 nm, irrespective of the salt concentration. Extrapolating the calculations to $\alpha = 0$ yields the pK of the intrinsic dissociation constant (pK_0) of about 3.2 (see Table 4), which is in reasonable agreement with data reported in the literature (3.0,[38] 3.4, 3.3[41]). The procedure used for the sample with ds = 0.75 was also applied to the other samples. It turns out that pK_0 does not depend on ds, provided the radius of the cylinder is taken as dependent on ds. Best fits were obtained using radii of 1.0, 1.05, and 1.15 nm for CMC with ds = 0.91, 0.99, and 1.25, respectively. This is not unreasonable, taking into account the size of a carboxymethyl group (which is estimated at 0.4 nm from atomic bond lengths) and the diameter of a glucose unit (0.50 nm[26]). Furthermore, the effective diameter of a cellulose chain is somewhat larger because a glucose molecule does not lie in line but is somewhat tilted with respect to its adjacent unit. Our conclusion that the cross-section of CMC increases with ds is corroborated by findings reported by Koda et al.[39] From density measurements on aqueous CMC (ds = 0.56−2.85) solutions with different concentrations they calculated the apparent molar volume. Extrapolation of these data to zero concentration yields the partial molar volume of CMC. The measurements in ref 39 reveal an increase of the partial molar volume with increasing ds, which is related to an increase in the dimension of the CMC backbone.

At this point we should comment on the validity of smearing-out discrete charges on the chain to a uniformly charged cylinder. Concerning the rigidity of the backbone the assumption is probably reasonable. As inferred from the SEC measurements, the polymer has a bare persistence length of about 15 nm. Hence, the polymer can be considered as stiff over a length of about 30 monomers. Thus, the assumption of a rigid backbone (cylinder) holds, even at high salt concentrations. An indication for the validity of the smearing-out can be found by comparing the distance between two charges with the radius of the Debye−Hückel ionic atmosphere around a charge on the chain. As stated by Muroga et al.[40] the assumption of a uniform charge density is not valid if the distance between two charged groups exceeds κ^{-1}. For CMC, the average distance between charged groups is given by $b/(\alpha ds)$. So the assumption maintains its validity as long as the degree of dissociation exceeds a critical value given by $\alpha_c = b/(\kappa^{-1} ds)$. In 0.01 mol L^{-1} NaCl (κ^{-1} = 3.04 nm) α_c = 0.23 and 0.14 for ds = 0.75 and 1.25, respectively. At this salt concentration experimental values always exceed the critical value. In 0.05 mol L^{-1} NaCl α_c is situated at 0.51 (ds = 0.75) and 0.30 (ds = 1.25), while α_c has values

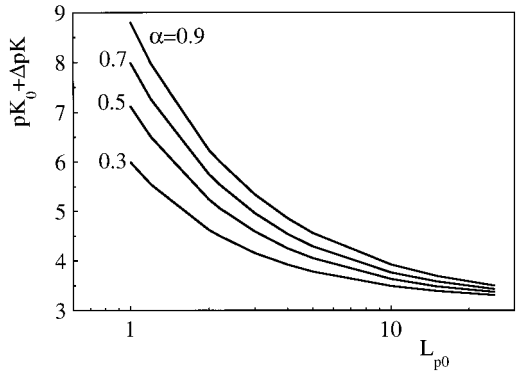

Figure 12. Calculated dissociation constant (pK_0 + ΔpK) of CMC ds = 0.75 in 0.01 mol L^{-1} 1:1 electrolyte as a function of L_{p0}. The curves were calculated for different degrees of dissociation α, using eq 12.

Table 5. Intrinsic Persistence Length Determined According to Katchalsky et al.[10,11,a]

ds	L_{p0}
0.75	5.6 ± 0.3
0.91	5.9 ± 0.5
0.99	6.1 ± 0.2
1.25	6.1 ± 0.3

[a] For all ds values, pK_0 was set to 3.2.

0.71 (ds = 0.75) to 0.43 (ds = 1.25) in 0.1 mol L^{-1} salt solution. For the higher salt concentrations the average distance is always below κ^{-1} (even for $\alpha = 1$) so the second requirement is not fulfilled. Thus we conclude that the model gives a satisfactory description of the polyelectrolyte if the salt concentration is in the range 0.01−0.1 mol L^{-1}. Indeed, the model predicts values of pK_0 in 0.5 and 1 mol L^{-1}, which differ considerable from the results obtained at lower salt concentrations.

In Figure 12 for CMC ds = 0.75, pK_0 + ΔpK calculated according to eq 12 (hence, by introducing discrete charges) is given as a function of the intrinsic persistence length at four degrees of ionization (α = 0.3, 0.5, 0.7, and 0.9) in 0.01 mol L^{-1} NaCl. The curves demonstrate that ΔpK decreases with the intrinsic persistence length. The origin of this dependence lies in the fact that in the model of Lifson and Katchalsky the charges are situated at the end of a Kuhn segment. As the intrinsic persistence length takes larger values, the average distance between two charges increases, eventually becoming infinite when L_{p0} goes to infinity. At very large separation the charges will not feel each other and, just like the change in electrostatic free energy, ΔpK converges to zero. From titration experiments, pK_0 + ΔpK at different degrees of dissociation is known. By comparing pK_0 + ΔpK calculated for fixed L_{p0}, but at different degrees of dissociation, with experiment, the plots in Figure 12 can be used to determine the value of L_{p0}. The result is given in Table 5, from which it can be seen that L_{p0} is not affected by ds. This result was also obtained from the SEC analyses. The magnitude of L_{p0}, however, is substantially lower than that according to the SEC analyses.

In Figure 13 pK_0 + ΔpK is given as a function of the degree of ionization for CMC with ds = 0.91 in 0.01 and 0.1 mol L^{-1} NaCl. Solid curves refer to the calculated ΔpK using eq 12 and taking L_{p0} = 5.8 and 3.5 nm for CMC in 0.01 and 0.1 mol L^{-1} NaCl, respectively. For comparison, data on xanthan in 0.01 mol L^{-1} NaCl[24] and CMC with ds = 0.81 in a salt free solution[41] are

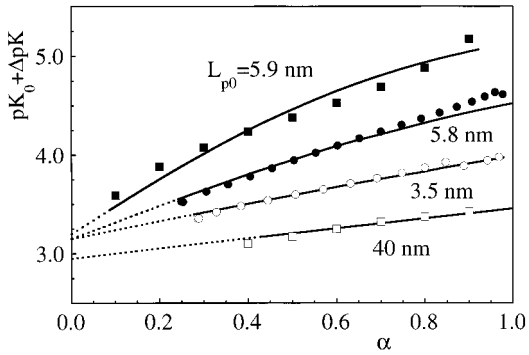

Figure 13. Apparent dissociation constant $pK_0 + \Delta pK$ as a function of degree of dissociation for CMC ds = 0.91 in 0.01 and 0.1 mol L^{-1} NaCl (symbols: ● and ○). The top curve (■) relates to CMC ds = 0.81 in salt free solution.[41] The lowest curve (□) is for xanthan in 0.01 mol L^{-1} NaCl.[24] Solid curves were calculated according to Katchalsky et al.[10,11] Best fits for L_{p0} are indicated in the figure.

also given. The low salt concentration data are derived from CMC titrations in the absence of salt, so the ionic strength (0.002 mol L^{-1}) is determined by the sodium counterions of NaCMC only. The figure shows that for the lower salt concentrations (0.002 and 0.01 mol L^{-1} NaCl) L_{p0} is predicted rather satisfactorily by Katchalsky's model at 5.8 nm. The same value is obtained at 0.05 mol L^{-1} NaCl. For higher salt concentrations L_{p0} is strongly underestimated. In 0.1 mol L^{-1} NaCl the model yields a value of $L_{p0} = 3.5$ nm; lower values were found at the highest salt concentrations. Probably this is caused by the assumption that charge interactions are accounted for by a Debye−Hückel interaction, which is not justified at high salt concentrations. For xanthan the best fit is obtained for $L_{p0} = 40$ nm, which corresponds to the bare persistence length of the single-helix conformation of the polymer.

In the derivation of eq 11, Katchalsky and Lifson evaluated the average value of $\exp(-\kappa r)/r$ using the probability function for the random configuration of an uncharged chain. For a charged molecule, compact configurations will occur less frequently than according to the random-chain probability function, which is a crude approximation. Thus, in the approach of Katchalsky and Lifson the electrostatic energy is overestimated. This probably causes a lower value of L_{p0} to be obtained with their model. Since the charges are assumed to be situated at the end of a Kuhn segment, increasing L_{p0} tends to decrease the electrostatic energy. Evaluating L_{p0} from potentiometric titrations by Katchalsky's theory cannot be considered an absolute method. However, it can be used satisfactorily for a reasonable estimate of L_{p0}.

Conclusions

CMC is characterized by means of SEC−MALLS and potentiometric titrations. The former method reveals information about the distribution of the molar mass and radius of gyration. R_g increases with decreasing electrolyte concentration, reflecting the influence of electrostatics on the dimension of the polymer. The dimension of CMC is described adequately with the electrostatic wormlike chain model.[8] Applying the model to the relation between M and R_g, an intrinsic persistence length of 16 nm is found for CMC, indicating that CMC can be seen as a semiflexible polymer. Odijk's model[9] for the swelling of polyelectrolytes yields a somewhat lower value ($L_{p0} \approx 12$ nm). The Davis theory[8] gives a more complete description as it takes molecular properties (such as the length and cross-section of the molecule) into account.

SEC−MALLS experiments show that the degree of substitution does not affect the relation between M and R_g. According to Odijk, this observation points to counterion condensation. Counterion condensation occurs when the average distance between charges becomes less than 0.714 nm (Bjerrum length); then counterions are kept in proximity of the polymer chain so that the effective average distance between charges equals the Bjerrum length. For fully dissociated CMC, counterion condensation takes place for ds > 0.75. In the Davis theory the charge density on the chain is calculated from the Poisson−Boltzmann equation for a uniformly charged cylinder. So, the relation between M and R_g is expected to depend on ds. However, if the cross-section of the backbone is taken into account, only a slight dependence is observed.

The cross-section (radius) of the CMC backbone was obtained from potentiometric titrations. Considering CMC as a uniformly charged cylinder, radii of 0.95 nm (ds = 0.75) up to 1.15 nm (ds = 1.25) were inferred. L_{p0} was also obtained from potentiometric titrations. Using Katchalsky's theory for the dissociation behavior as a function of the polymer stiffness, L_{p0} was found to be 5.9 nm. That this value is lower than that inferred from SEC−MALLS is probably due to an incorrect evaluation of the electrostatic energy in the Katchalsky model. Potentiometric titrations are experimentally less time consuming than SEC−MALLS. However, taking into account the shortcomings of the model, they can serve at best as a suitable technique to estimate the persistence length of a polyelectrolyte.

Acknowledgment. This work was carried out with financial support of the Dutch National Innovation Oriented Program Carbohydrates (IOP-k).

Appendix

In this appendix we briefly outline the numerical procedure that is used for the calculation of the potential at the surface of the polyelectrolyte chain. Besides ψ_0 the procedure yields the relation between λ and λ_{eff}.

The Poisson−Boltzmann equation for a uniformly charged cylinder in a solution containing a 1:1 electrolyte in cylindrical coordinates is given by

$$\frac{1}{r}\frac{\mathrm{d}}{\mathrm{d}r}\, r\frac{\mathrm{d}\psi(r)}{\mathrm{d}r} = -\frac{\rho_c(r)}{\epsilon_0\epsilon_r} = \kappa^2\frac{kT}{q_e}\sinh\left(\frac{q_e}{kT}\psi(r)\right) \quad \text{(A1)}$$

where $\rho_c(r)$ is the charge density and $\psi(r)$ is the potential at distance r from the center of the cylinder. Introducing dimensionless variables u and Ψ by means of $u = \ln(\kappa^{-1}r)$ and $\Psi = q_e\psi/kT$, we can rewrite eq A1 in terms of two coupled first-order differential equations:[23]

$$\frac{\mathrm{d}\Psi}{\mathrm{d}u} = z \quad \text{(A2)}$$

$$\frac{\mathrm{d}z}{\mathrm{d}u} = \mathrm{e}^{2u}\sinh(\Psi) \quad \text{(A3)}$$

This set of equations is solved numerically via a fourth-order Fehlberg algorithm.[42] First, a values is assigned

to λ_{eff}. The integration starts at a large distance from the surface ($\rho = 10$), where the linearized solution (i.e., at a large distance where Ψ is low) of the PB equation is applicable:

$$\Psi = 2\lambda_{eff}K_0(e^u)/[(a + d)\kappa K_1((a + d)\kappa)] \quad \text{(A4)}$$

$$z = -2\lambda_{eff}e^u K_1(e^u)/[(a + d)\kappa K_1((a + d)\kappa)] \quad \text{(A5)}$$

K_0 and K_1 are modified Bessel functions of the second kind of order zero and one, respectively. The integration proceeds inward until $r = a + d$. The potential and charge density at the boundary of the Stern layer are determined as $\psi_{a+d} = \psi$ and $\lambda = -1/2z$ at $r = a + d$.[23] In this manner, one can calculate for each value of λ_{eff} a corresponding value of λ, so that a relation between the charge density and the effective charge density is obtained. Finally, with the use of the expression for the capacitance of a cylindrical capacitor, the surface potential is calculated, yielding the relation between λ and ψ_0.

References and Notes

(1) Fleer, G. J.; Cohen Stuart, M. A.; Scheutjens, J. M. H. M.; Cosgrove, T.; Vincent, B. *Polymers at Interfaces*; Chapman & Hall: London, 1993; p 33.
(2) Yalpani, M. *Polysaccharides*; Elsevier: New York, 1988.
(3) Rinaudo, M. In *Cellulose and cellulose derivatives: Physicochemical aspects and industrial applications*; Kennedy, J. F., Phillips, G. O., Williams, P. O., Piculell, L., Eds.; Woodhead Publishing Limited: Cambridge, U.K., 1995; p 257.
(4) Yamakawa, H.; Fujii, M. *Macromolecules* **1974**, *7*, 128.
(5) Kamide, K.; Saito, M.; Suzuki, H. *Makromol. Chem., Rapid Commun.* **1983**, *44*, 33.
(6) Benoit, H.; Doty, P. M. *J. Phys. Chem.* **1953**, *57*, 958.
(7) Lavrenko, P. N.; Okatova, O. V.; Tsvetkov, V. N.; Dautzenberg, H.; Philipp, B. *Polymer* **1990**, *31*, 348.
(8) Davis, R. M. *Macromolecules* **1991**, *24*, 1149.
(9) Odijk, T. *Biopolymers* **1979**, *18*, 3111.
(10) Katchalsky, A.; Shavit, N.; Eisenberg, H. *J. Polym. Sci.* **1954**, *13*, 69.
(11) Katchalsky, A.; Lifson, S. *J. Polym. Sci.* **1954**, *13*, 43.
(12) Katchalsky, A.; Lifson, S. *J. Polym. Sci.* **1951**, *11*, 409.
(13) Kuhn, W. *Kolloid Z.* **1934**, *68*, 2.
(14) Yamakawa, H. *Modern Theory of Polymer Solutions*; Harper & Row: New York, 1971; (a) p 56, (b) p 108.
(15) Yamakawa, H.; Stockmayer, W. *J. Chem. Phys.* **1972**, *57*, 2843.
(16) Davis, R. M.; Russel, W. B. *J. Polym. Sci., Polym. Phys.* **1986**, *24*, 511.
(17) Odijk, T. *Macromolecules* **1979**, *12*, 688.
(18) Skolnick, J.; Fixman, M. *Macromolecules* **1977**, *10*, 944.
(19) Odijk, T.; Houwaart, A. C. J. *Polym. Sci., Polym. Phys. Ed.* **1978**, *16*, 627.
(20) Fixman, M.; Skolnick, J. *Macromolecules* **1978**, *11*, 863.
(21) Manning, G. S. *J. Chem. Phys.* **1969**, *51*, 924.
(22) Fixman, M. *J. Chem. Phys.* **1979**, *70*, 4995.
(23) Russel, W. B. *J. Polym. Sci.* **1982**, *20*, 1233.
(24) Zhang, L.; Takematsu, T.; Norisuye, T. *Macromolecules* **1987**, *20*, 2882.
(25) Zimm, B. *J. Chem. Phys.* **1948**, *16*, 1093.
(26) Ott, E.; Spurlin, H. M.; Grafflin, M. W. *Cellulose and Cellulose Derivatives part II*; High Polymers, Vol. V; Interscience Publishers: New York, 1954; p 676.
(27) Reuben, J.; Connor, H. T. *Carbohydr. Res.* **1983**, *115*, 1.
(28) Buytenhuys, F. A.; Bonn, R. *Papier (Darmstadt)* **1977**, *31*, 525.
(29) Ma, Z.; Wiebang, Z.; Li, Z. *Chinese J. Polym. Sci.* **1989**, *7*, 45.
(30) Shortt, D. W. *J. Liq. Chromatogr.* **1993**, *16*, 3371.
(31) *CRC Standard Probability and Statistics, Tables and Formulae*; Beyer, W. H., Ed.; CRC Press: Boston, 1991; p 231.
(32) Mijnlieff, P. F.; Coumou, D. J. *J. Colloid Interface Sci.* **1968**, *27*, 553.
(33) Struszczyk, H.; Wrzesniewka-Tosik, K.; Ciechanska, D.; Wesolowska, E. In *Cellulose and Cellulose derivatives: Physicochemical aspects and industrial applications*; Kennedy, J. F., Phillips, G. O., Williams, P. O., Piculell, L., Eds.; Woodhead Publishing Limited: Cambridge, U.K., 1995.
(34) de Gennes, P. G. *Scaling Concepts in Polymer Physics*; Cornell University Press: Ithaca, NY, 1979.
(35) Schulz, L.; Burchard, W. *Das Papier* **1993**, *42*, 1.
(36) de Nooy, A. E. J.; Besemer, A. C.; van Bekkum, H.; van Dijk, J. A. P. P.; Smit, J. A. M. *Macromolecules* **1996**, *29*, 6541.
(37) Millero, F. J. *Chem. Rev.* **1971**, *71*, 147.
(38) Rinaudo, M. In *Polyelectrolytes*; Sélégny, E., Mandel, M., Strauss, U. P., Eds.; Charged and Reactive Polymers, Vol. I; D. Reidel Publishing Co.: Dortrecht, The Netherlands, 1994; p 163.
(39) Koda, S.; Hasegawa, S.; Mikuriya, M.; Kawaizumi, F.; Nomura, H. *Polymer* **1988**, *29*, 2100.
(40) Muroga, Y.; Suzuki, K.; Kawaguchi, Y.; Nagasawa, M. *Biopolymers* **1972**, *11*, 137.
(41) Crowdhury, F. H.; Neale, S. M. *J. Polym. Sci. A* **1963**, *1*, 2881.
(42) Press, W. H.; Teukolsky, S. A.; Vetterling, W. T. *Numerical Recipes*; Cambridge University Press: New York, 1989; p 552.

MA971032I